Supporting Information

Nanosized Mo-doped CeO_2 enhances the electrocatalytic property of the Pt anode catalyst in direct methanol fuel cells

Genlei Zhang[a, §], Zhenzhen Yang[a, §], Wen Zhang[a], Yuxin Wang[a, *]

[a]School of Chemical Engineering and Technology, State Key Laboratory of Chemical Engineering, Co-Innovation Center of Chemical Science & Engineering, Tianjin Key Laboratory of Membrane Science and Desalination Technology, Tianjin University, Tianjin, 300350, PR China. E-mail: yxwang@tju.edu.cn; Tel: +86-22-27890515

Supporting Tables and Figures

Table S1 Lattice parameter of Pt, actual Pt loading, ECSA, onset potential and mass activity of Pt/CeO_2-C, $Pt/Ce_{1-x}Mo_xO_{2-\delta}$-C, Pt/C-H and Pt/C-JM catalysts, respectively.

Sample	Lattice parameter of Pt / nm	Actual Pt loading / %	ECSA / $m^2\ g^{-1}$	Onset potential / mV *vs* SCE	Mass activity / $mA\ mg_{Pt}^{-1}$
Pt/CeO_2-C	0.3917	18.7	73.19	381	951.8
$Pt/Ce_{0.8}Mo_{0.2}O_{2-\delta}$-C	0.3901	18.9	83.59	376	1197.7
$Pt/Ce_{0.7}Mo_{0.3}O_{2-\delta}$-C	0.3892	18.9	94.01	372	1888.4
$Pt/Ce_{0.6}Mo_{0.4}O_{2-\delta}$-C	0.3909	18.8	86.54	365	1506.7
Pt/C-H	0.3923	18.6	41.97	448	136.7
Pt/C-JM	-	19.8	52.89	427	418.2

Table S2 The peak area ratio in the Raman spectra, actual atomic ratio of Ce/Mo, BET surface area, electronic conductivity, the proportions of Ce^{3+} and O_C of pure CeO_2 and Mo-doped CeO_2 samples, respectively.

Sample	$(A_I + A_{III})/A_{II}$	Actual Ce/Mo	BET / $m^2\ g^{-1}$	Electronic conductivity / S cm^{-1}	$Ce^{3+}/(Ce^{3+}+Ce^{4+})$ / %$^{\alpha}$	$O_C/(O_C+O_L)$ / %$^{\beta}$
CeO_2	0.0316	1:0	53	1.3×10^{-4}	11.24	25.6
$Ce_{0.8}Mo_{0.2}O_{2-\delta}$	0.113	1.8/8.2	145	1.8×10^{-2}	11.89	44.3
$Ce_{0.7}Mo_{0.3}O_{2-\delta}$	0.245	2.9/7.1	156	0.15	12.27	55.2
$Ce_{0.6}Mo_{0.4}O_{2-\delta}$	0.328	3.8/5.2	168	0.23	12.65	58.7

$^{\alpha, \beta}$ calculated from XPS

Table S3 The positive scan peak current density normalized as mass activity for the $Pt/Ce_{0.7}Mo_{0.3}O_{2-\delta}$-C catalyst and other recently reported catalysts.

Catalyst	Mass activity / mA mg_{Pt}^{-1}	Scanning rate / mV/s	Condition	References
$Pt/Ce_{0.7}Mo_{0.3}O_{2-\delta}$-C	1888.4	50	0.5 M H_2SO_4 + 1 M CH_3OH	This work
Pt/C-MoC-Gl	1596.7	50	0.5 M H_2SO_4 + 1 M CH_3OH	[1]
Pt-Ni_2P/C-30%	1432	50	0.5 M H_2SO_4 + 1 M CH_3OH	[2]
Pt/I-IL (10)/GNPs	1559.7	50	0.5 M H_2SO_4 + 1 M CH_3OH	[3]
Pt/MnO_x-MWCNTs	1367.3	50	0.5 M H_2SO_4 + 1 M CH_3OH	[4]
Pt/MnO_2/GS	1224	20	1 M H_2SO_4 + 2 M CH_3OH	[5]
Pt-SiO2/graphene	1047	50	0.5 M H_2SO_4 + 1 M CH_3OH	[6]
$Pt/Ce_{0.8}Sn_{0.2}O_{2-\delta}$-C	502	50	0.5 M H_2SO_4 + 0.5 M CH_3OH	[7]
$Pt/Ti_{0.9}Sn_{0.1}O_2$-C	459.6	10	0.5 M H_2SO_4 + 0.5 M CH_3OH	[8]
Pt/CeO_2/graphene	366	100	0.5 M H_2SO_4 + 1 M CH_3OH	[9]
Pt/CeO_2/PANI	361.33	100	0.5 M H_2SO_4 + 0.5 M CH_3OH	[10]
Pt/TiO_2@N-doped C-900	490	50	0.5 M H_2SO_4 + 1 M CH_3OH	[11]
Pt-MoO_x/CNTs	246.2	20	0.5 M H_2SO_4 + 1 M CH_3OH	[12]
Pt/TiO_2-C	102.8	50	0.5 M H_2SO_4 + 0.5 M CH_3OH	[13]

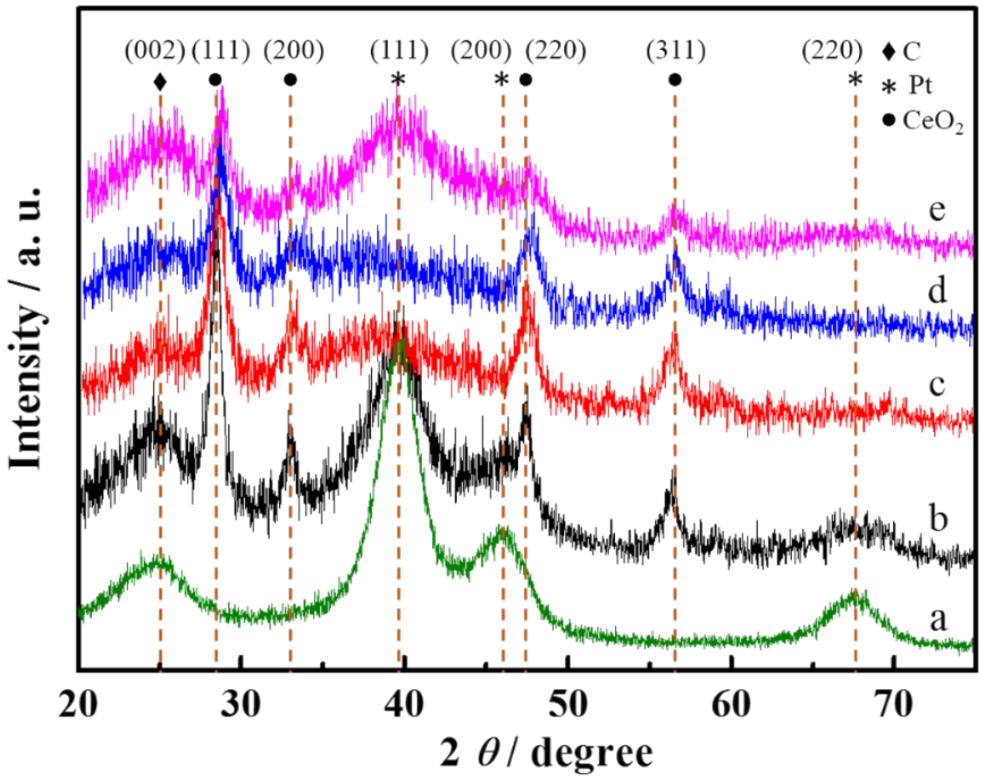

Figure S1 XRD patterns of (a) Pt/C-H, (b) Pt/CeO_2-C (b), (c) Pt/$Ce_{0.8}Mo_{0.2}O_{2-\delta}$-C, (d) Pt/$Ce_{0.7}Mo_{0.3}O_{2-\delta}$-C and (e) Pt/$Ce_{0.6}Mo_{0.4}O_{2-\delta}$-C catalysts.

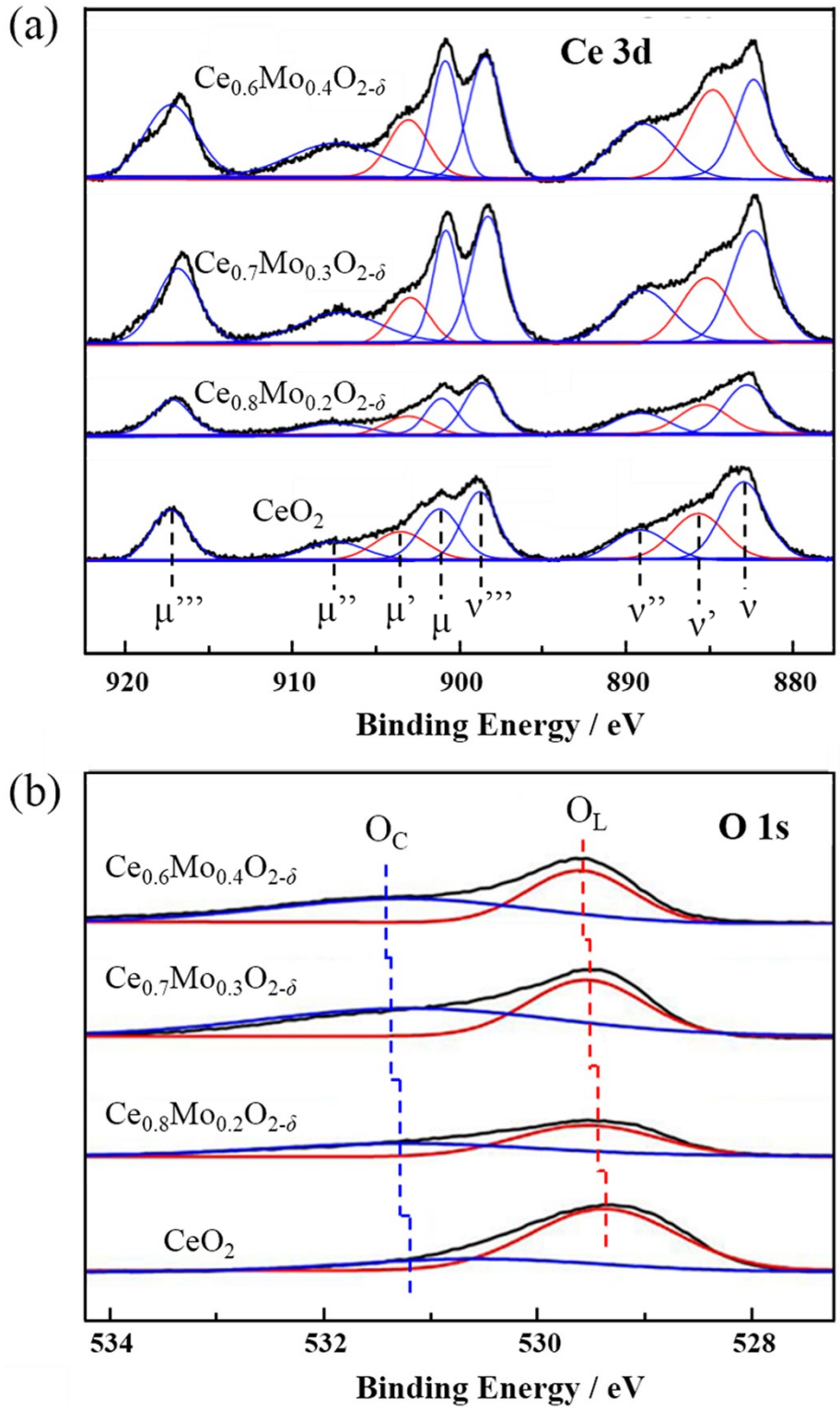

Figure S2 XPS spectra of (a) Ce 3d and (b) O 1s for CeO_2 and $Ce_{1-x}Mo_xO_{2-\delta}$.

XPS was performed in order to further illuminate the surface composition and the chemical state of the elements existing in Mo-doped CeO_2 samples with various Mo doping ratios. The XPS results of Ce 3d for CeO_2 and $Ce_{1-x}Mo_xO_{2-\delta}$ are shown in Figure

S2a. The bands labeled μ, μ'', μ''', ν, ν'' and ν''' represent the $3d^{10}4f^0$ state of Ce^{4+}, whereas μ' and ν' represent the $3d^{10}4f^1$ state, corresponding to Ce^{3+}. The presence of Ce^{3+} is due to the reduction of Ce^{4+} in the oxide structure.[14] The fraction of Ce^{3+} species can be estimated using relative areas of ν' and μ' peaks according to the equation:

$$[Ce^{3+}] = \frac{S_{\nu'} + S_{\mu'}}{\Sigma(S_\nu + S_\mu)}$$

where S is the integrated area corresponding to peak ν^i or μ^I. The calculated ratios of Ce^{3+} for the CeO_2, $Ce_{0.8}Mo_{0.2}O_{2-\delta}$, $Ce_{0.7}Mo_{0.3}O_{2-\delta}$ and $Ce_{0.6}Mo_{0.4}O_{2-\delta}$ are 11.24, 11.89, 12.27 and 12.65 %, respectively. Therefore, the relative content for Ce^{3+} in the oxides increased after increasing the doping level of Mo.

The XPS spectra of O 1s for CeO_2 and $Ce_{1-x}Mo_xO_{2-\delta}$ are shown in Figure S2b. The O1s XPS spectra appear broad, which can be deconvoluted into two distinct peaks, referred to as the lattice oxygen (O_L) at about 529.3 eV and the chemisorbed surface oxygen (O_C) at about 531.2 eV. The strong peaks of the samples at about 531.2 eV suggest that they are expected to have better OSC, which would be promising for their highly active in oxidation reactions. The ratios of O_C for CeO_2, $Ce_{0.8}Mo_{0.2}O_{2-\delta}$, $Ce_{0.7}Mo_{0.3}O_{2-\delta}$ and $Ce_{0.6}Mo_{0.4}O_{2-\delta}$ are 25.6, 44.3, 55.2 and 58.7 %, respectively, indicating that the content of surface oxygen vacancy is increased after increasing the doping ratio of Mo.

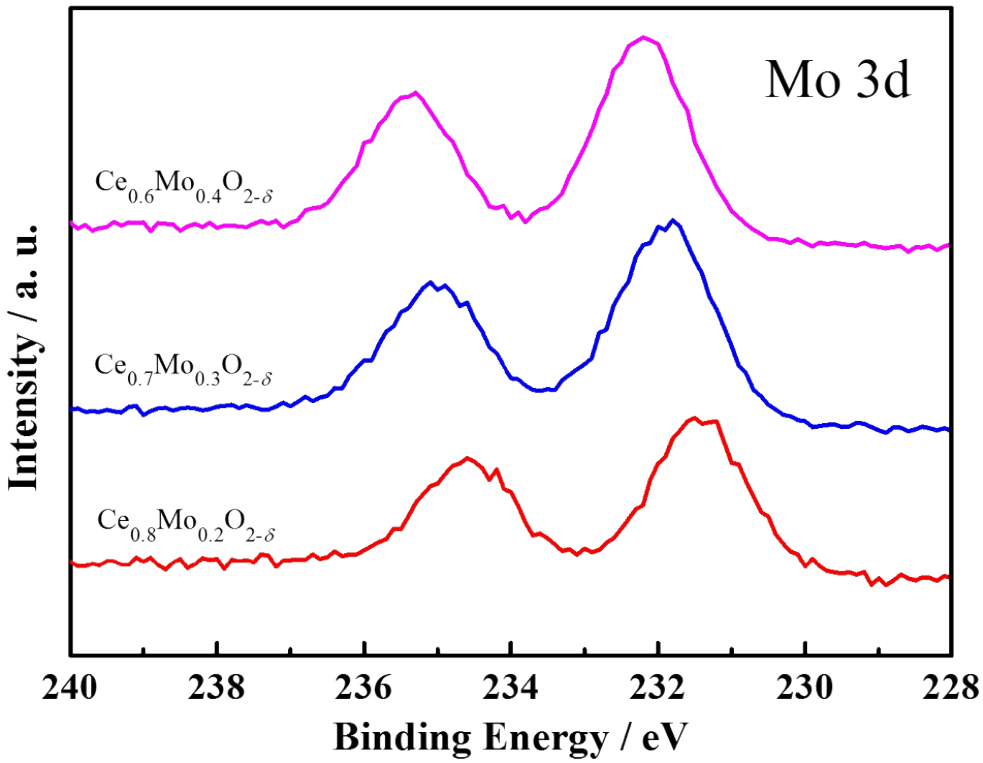

Figure S3 XPS spectra of Mo 3d for $Ce_{0.8}Mo_{0.2}O_{2-\delta}$, $Ce_{0.7}Mo_{0.3}O_{2-\delta}$, $Ce_{0.6}Mo_{0.4}O_{2-\delta}$ solid solutions.

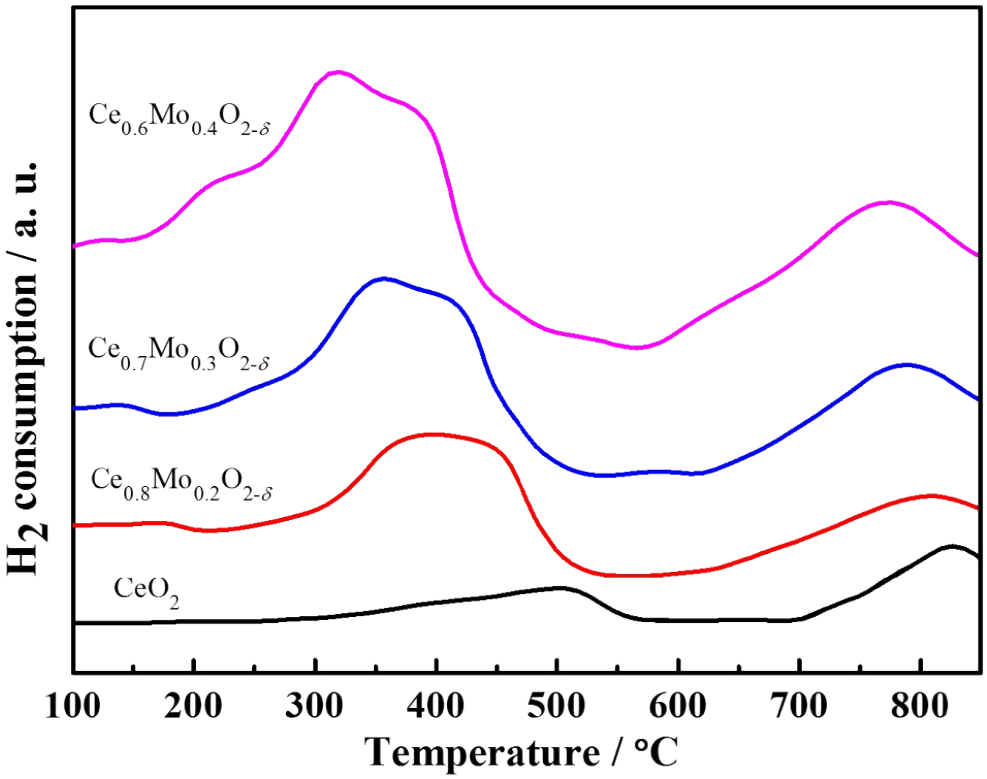

Figure S4 TPR profiles of CeO_2 and $Ce_{1-x}Mo_xO_{2-\delta}$.

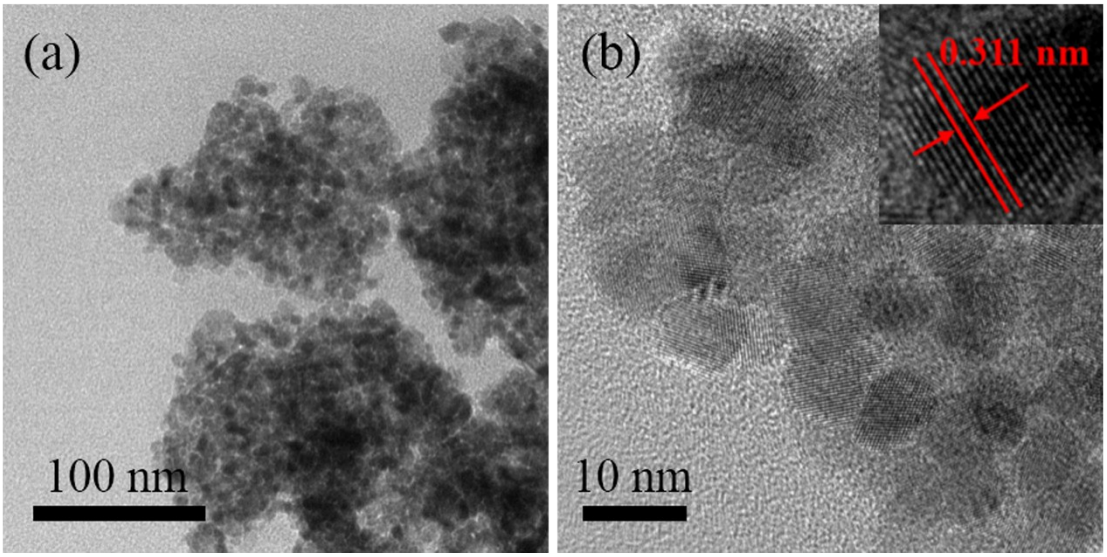

Figure S5 (a) TEM and (b) HRTEM images of CeO_2.

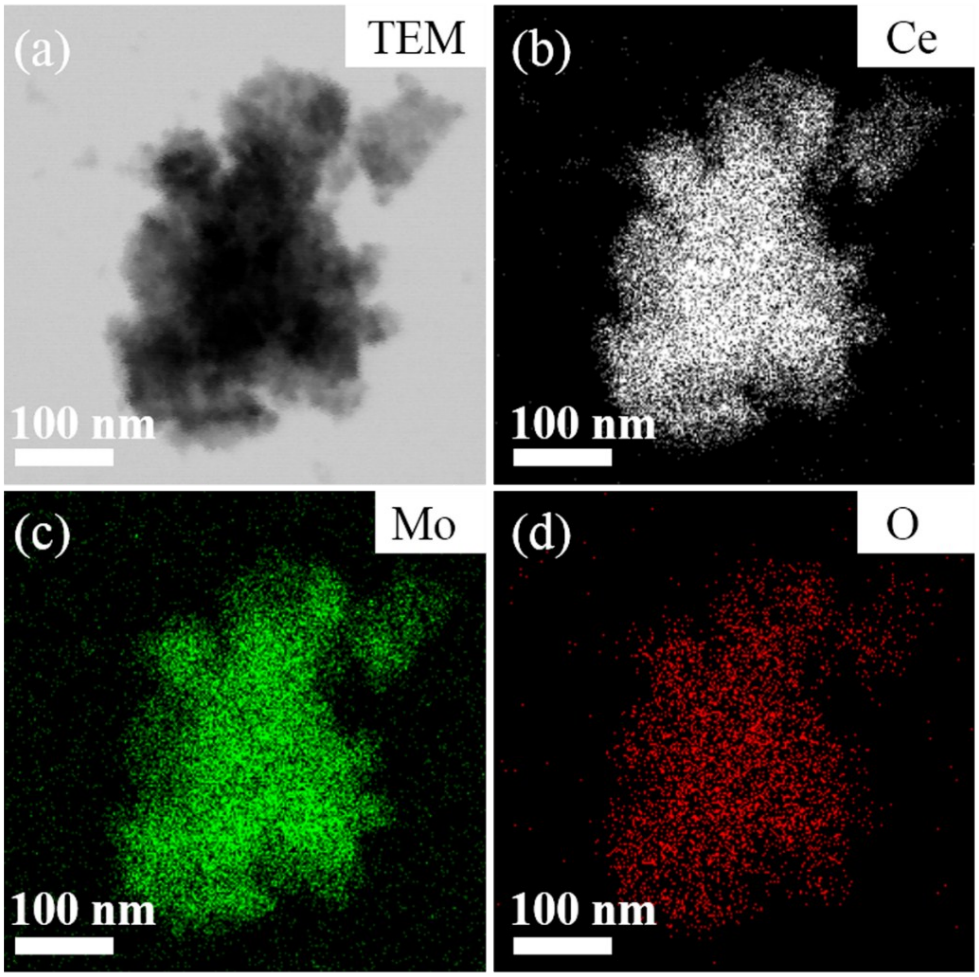

Figure S6 (a) TEM, (b-d) Elemental mapping images of the $Ce_{0.7}Mo_{0.3}O_{2-\delta}$.

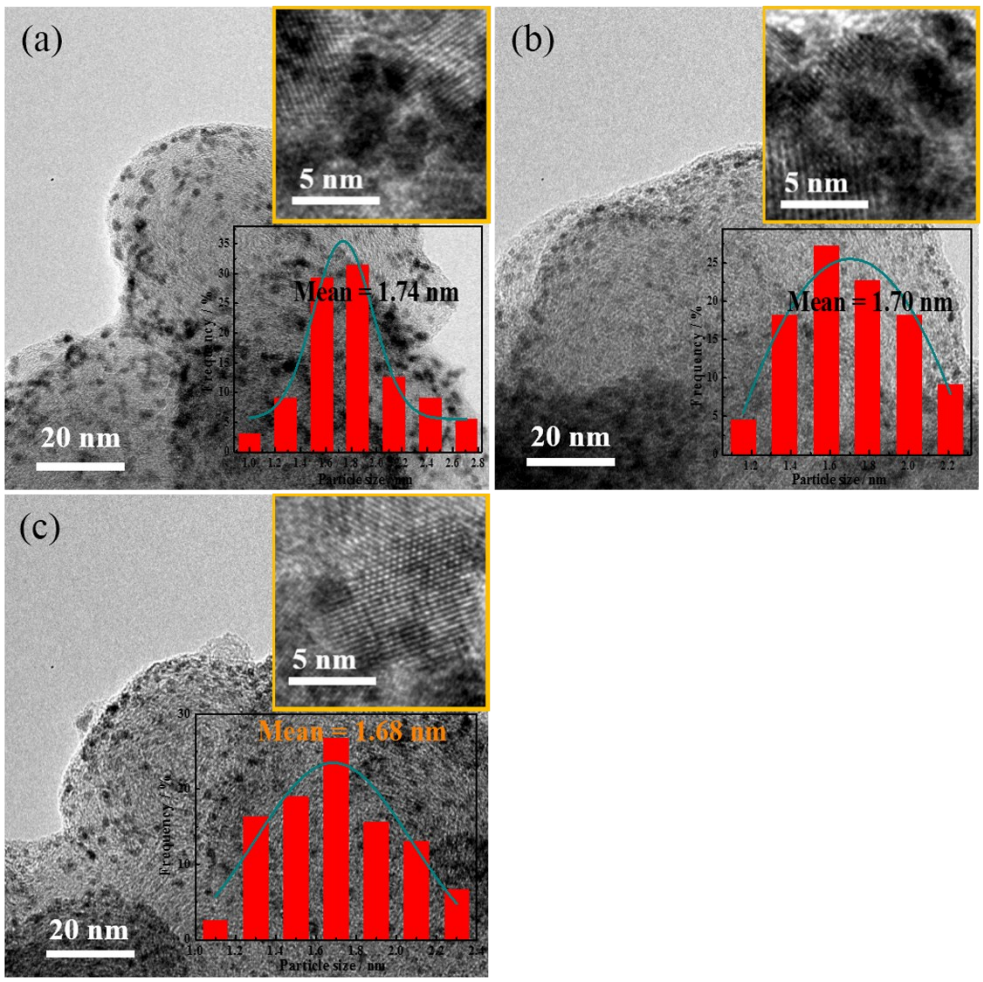

Figure S7 TEM, HRTEM images and the Pt particle size distribution of (a) Pt/CeO_2-C, (b) Pt/$Ce_{0.8}Mo_{0.2}O_{2-\delta}$-C and (c) Pt/$Ce_{0.6}Mo_{0.4}O_{2-\delta}$-C catalysts.

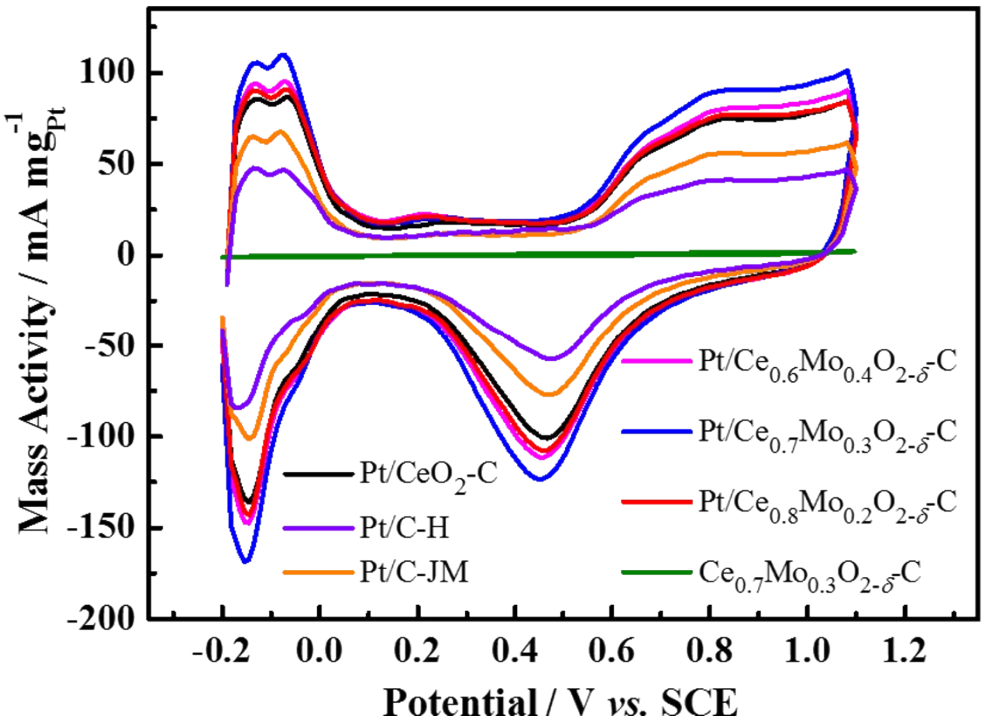

Figure S8 Typical CVs of Pt/CeO_2-C, Pt/$Ce_{0.8}Mo_{0.2}O_{2-\delta}$-C, Pt/$Ce_{0.7}Mo_{0.3}O_{2-\delta}$-C, Pt/$Ce_{0.6}Mo_{0.4}O_{2-\delta}$-C, $Ce_{0.7}Mo_{0.3}O_{2-\delta}$-C, Pt/C-H and Pt/C-JM catalysts in 0.5 M H_2SO_4.

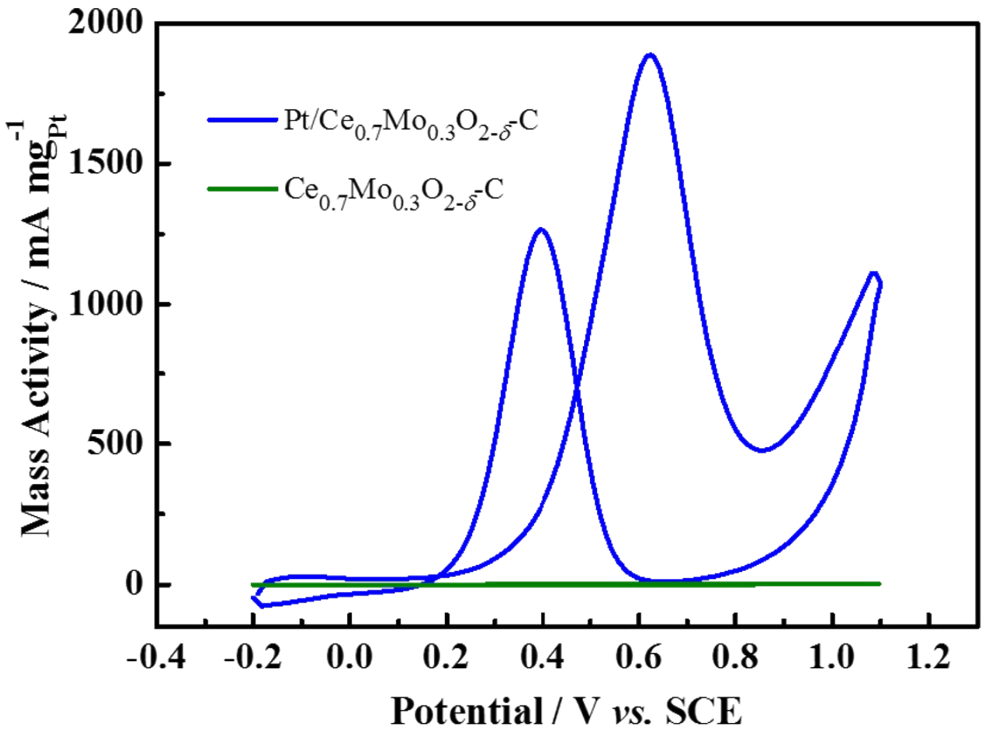

Figure S9 Typical CVs of Pt/$Ce_{0.7}Mo_{0.3}O_{2-\delta}$-C and $Ce_{0.7}Mo_{0.3}O_{2-\delta}$-C in 0.5 M H_2SO_4 solution containing 1 M CH_3OH.

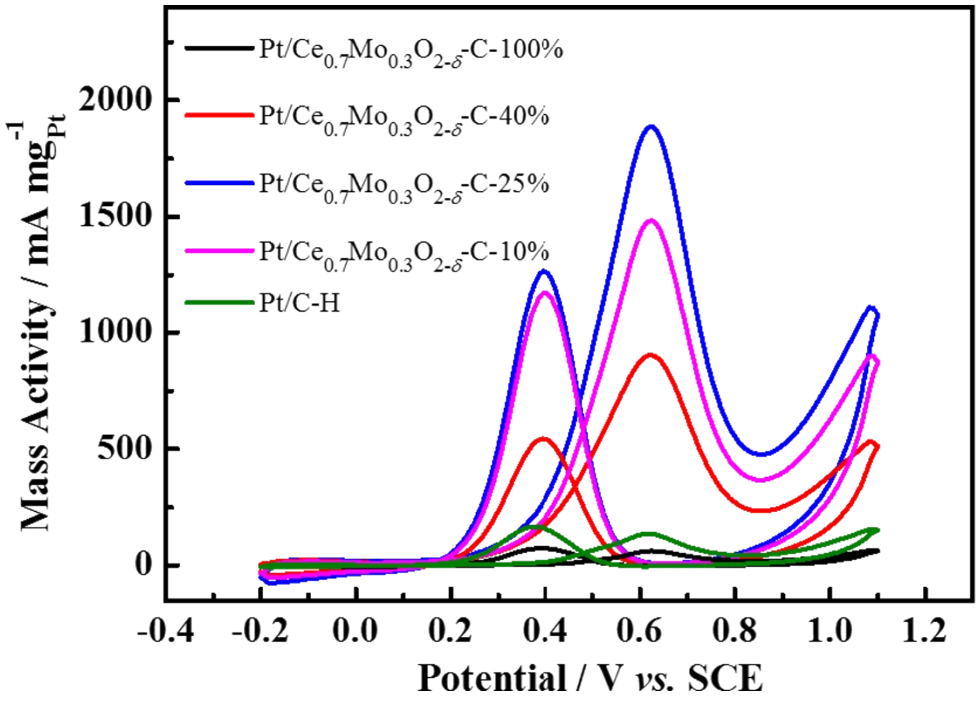

Figure S10 Typical CVs of $Pt/Ce_{0.7}Mo_{0.3}O_{2-\delta}$-C catalysts with various loadings of $Ce_{0.7}Mo_{0.3}O_{2-\delta}$ in 0.5 M H_2SO_4 solution containing 1 M CH_3OH.

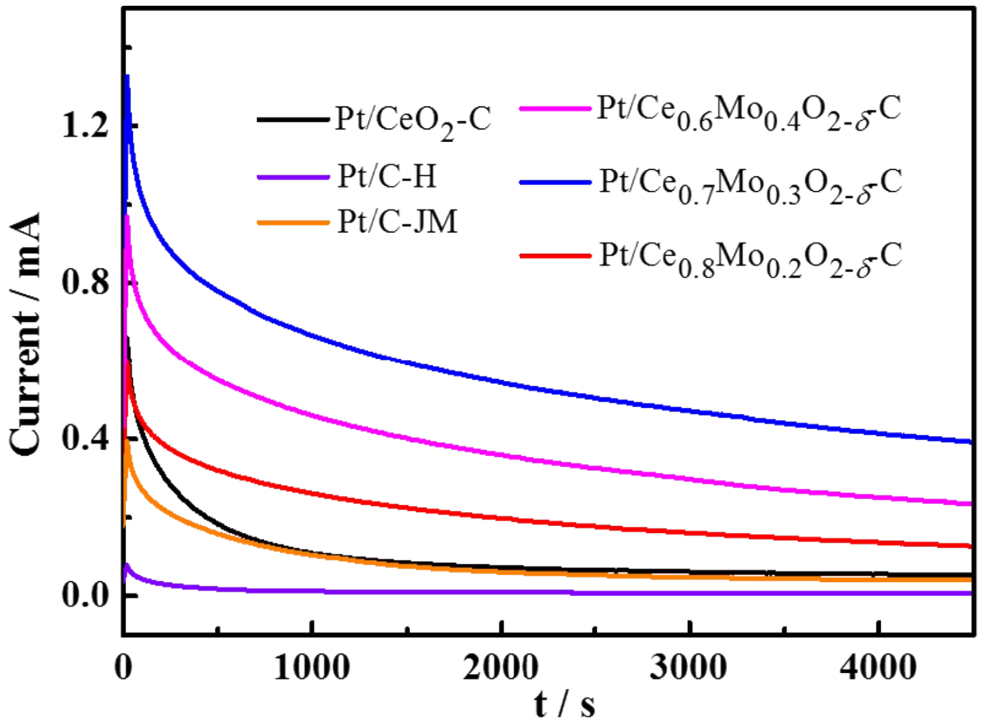

Figure S11 CA curves of Pt/CeO_2-C, $Pt/Ce_{0.8}Mo_{0.2}O_{2-\delta}$-C, $Pt/Ce_{0.7}Mo_{0.3}O_{2-\delta}$-C, $Pt/Ce_{0.6}Mo_{0.4}O_{2-\delta}$-C, Pt/C-H and Pt/C-JM catalysts in 0.5 M H_2SO_4 solution containing 1 M CH_3OH at 0.6 V for 4500 s.

References

1. Z. Yan, G. He, P. K. Shen, Z. Luo, J. Xie and M. Chen, *J. Mater. Chem. A*, 2014, **2**, 4014-4022.
2. J. Chang, L. Feng, C. Liu, W. Xing and X. Hu, *Energy Environ. Sci.*, 2014, **7**, 1628-1632.
3. G. Zhang, Z. Yang, C. Huang, W. Zhang and Y. Wang, *Nanoscale*, 2015, **7**, 10170-10177.
4. A. Nouralishahi, A. A. Khodadadi, Y. Mortazavi, A. Rashidi and M. Choolaei, *Electrochim. Acta*, 2014, **147**, 192-200.
5. H. Huang, Q. Chen, M. He, X. Sun and X. Wang, *J. Power Sources*, 2013, **239**, 189-195.
6. T. H. T. Vu, T. T. T. Tran, H. N. T. Le, L. T. Tran, P. H. T. Nguyen, H. T. Nguyen and N. Q. Bui, *Electrochim. Acta*, 2015, **161**, 335-342.
7. Y. Gu, C. Liu, Y. Li, X. Sui, K. Wang and Z. Wang, *J. Power Sources*, 2014, **265**, 335-344.
8. Y. Li, C. Liu, Y. Liu, B. Feng, L. Li, H. Pan, W. Kellogg, D. Higgins and G. Wu, *J. Power Sources*, 2015, **286**, 354-361.
9. X. Wang, X. Li, D. Liu, S. Song and H. Zhang, *Chem. Commun.*, 2012, **48**, 2885-2887.
10. H. Xu, A. L. Wang, Y. Tong and G. R. Li, *ACS Catal.*, 2016, **6**, 5198-5206.
11. X. Zhao, J. Zhu, L. Liang, J. Liao, C. Liu and W. Xing, *J. Mater. Chem.*, 2012, **22**, 19718-19725.
12. Z. M. Cui, S. P. Jiang and C. M. Li, *Chem. Commun.*, 2011, **47**, 8418-8420.
13. Y. Fan, Z. Yang, P. Huang, X. Zhang and Y. M. Liu, *Electrochim. Acta*, 2013, **105**, 157-161.
14. J. Hierso, O. Sel, A. Ringuede, C. Laberty-Robert, L. Bianchi, D. Grosso and C. Sanchez, *Chem. Mater.*, 2009, **21**, 2184-2192.